Published in final edited form as:

AJR Am J Roentgenol. 2015 December ; 205(6): 1208–1214. doi:10.2214/AJR.15.14482.

Prostate Cancer: Utility of Whole-Lesion Apparent Diffusion Coefficient Metrics for Prediction of Biochemical Recurrence After Radical Prostatectomy

Andrew B. Rosenkrantz[1], **Justin M. Ream**[1], **Paul Nolan**[1], **Henry Rusinek**[1], **Fang-Ming Deng**[2], and **Samir S. Taneja**[3]

[1]Department of Radiology, Center for Biomedical Imaging, NYU School of Medicine, NYU Langone Medical Center, 660 First Ave, 3rd Fl, New York, NY 10016

[2]Department of Pathology, NYU School of Medicine, NYU Langone Medical Center, New York, NY

[3]Department of Urology, Division of Urologic Oncology, NYU School of Medicine, NYU Langone Medical Center, New York, NY

Abstract

OBJECTIVE—The purpose of this study was to investigate the additional value of whole-lesion histogram apparent diffusion coefficient (ADC) metrics, when combined with standard pathologic features, in prediction of biochemical recurrence (BCR) after radical prostatectomy for prostate cancer.

MATERIALS AND METHODS—The study included 193 patients (mean age, 61 ± 7 years) who underwent 3-T MRI with DWI (b values, 50 and 1000 s/mm^2) before prostatectomy. Histogram metrics were derived from 3D volumes of interest encompassing the entire lesion on ADC maps. Pathologic features from radical prostatectomy and subsequent BCR were recorded for each patient. The Fisher exact test and Mann-Whitney test were used to compare ADC-based metrics and pathologic features between patients with and patients without BCR. Stepwise logistic regression analysis was used to construct multivariable models for prediction of BCR, which were assessed by ROC analysis.

RESULTS—BCR occurred in 16.6% (32/193) of patients. Variables significantly associated with BCR included primary Gleason grade, Gleason score, extraprostatic extension, seminal vesicle invasion, positive surgical margin, preoperative prostate-specific antigen level, MRI tumor volume, mean whole-lesion ADC, entropy ADC, and mean ADC of the bottom 10th, 10–25th, and 25–50th percentiles ($p \leq 0.019$). Significant independent predictors of BCR at multivariable analysis were primary Gleason grade, extraprostatic extension, mean of the bottom 10th percentile ADC, and entropy ADC ($p = 0.002$–0.037). The AUC of this multivariable model was 0.94 for prediction of BCR; the AUC of pathologic features alone was 0.89 ($p = 0.001$).

Address correspondence to A. B. Rosenkrantz (Andrew.Rosenkrantz@nyumc.org).

Based on a presentation at the Society of Abdominal Radiology 2015 annual meeting, Coronado, CA.

CONCLUSION—A model integrating whole-lesion ADC metrics had significantly higher performance for prediction of BCR than did standard pathologic features alone and may help guide postoperative prognostic assessments and decisions regarding adjuvant therapy.

Keywords

apparent diffusion coefficient; DWI; MRI; prostate cancer; radical prostatectomy

Radical prostatectomy for the management of localized prostate cancer is associated with a substantial reduction in mortality [1]. The serum prostate-specific antigen (PSA) level is generally undetectable postoperatively, consistent with removal of the entire prostate and any tumor. However, a minority of patients have measurable PSA after surgery, which constitutes biochemical recurrence (BCR) of disease [2]. BCR is associated with increased risk of metastatic disease and prostate cancer–specific mortality [3, 4]. Therefore, documented BCR without distant metastatic disease typically warrants treatment with salvage pelvic radiation, possibly with concomitant hormonal therapy, to improve survival [5–7]. In addition, in patients at high risk of BCR because of the pathologic findings at prostatectomy, adjuvant pelvic radiation may be provided postoperatively to reduce the risk of subsequent BCR [8–10]. Therefore, reliable prediction of BCR is important for providing the patient accurate prognostic information and making optimal treatment decisions.

To facilitate prediction of BCR, extensive efforts have been dedicated to development of clinical nomograms [11–13]. These models incorporate numerous clinical and pathologic parameters and complex interactions among such parameters to provide an individualized estimate of the likelihood of a given outcome [14]. In prediction of BCR, established postoperative nomograms have incorporated preoperative PSA level, Gleason score, tumor stage, tumor size, surgical margin status, and other features. These models have become widely adopted in clinical practice and decision making. Nonetheless, their performance remains suboptimal, and novel complementary biomarkers, such as those based on genetic profiling of tumors, are under active investigation [15]. Therefore, a means of improving the predictive accuracy of multivariate models for BCR would be of great clinical importance.

The apparent diffusion coefficient (ADC) value of prostate cancer, derived through DWI, has been found in numerous studies to have statistically significant correlation with the Gleason score of the tumor [16–18] and to be associated with tumor stage and progression in both active surveillance and radiation therapy cohorts. On this basis, ADC has come to be recognized as a key marker of the aggressiveness of prostate cancer. One past study [19] showed ADC to be predictive of BCR. In that study, however, no other clinical or pathologic features were observed to be significant independent predictors of BCR, and therefore no multivariate model could be constructed [19]. The overall accuracy of ADC alone as a single-factor predictor of BCR was similar to that of previously established clinical nomograms [14]. Since that study, more sophisticated ADC metrics have been found to have additive value as markers of tumor grade. Specifically, histogram-based whole-lesion ADC metrics have had stronger associations than mean ADC with Gleason score or primary Gleason grade [20, 21]. Such metrics have the potential to further improve on the role of ADC values in prediction of BCR. Our aim in this study was to investigate the

additional value of whole-lesion histogram ADC metrics combined with standard pathologic features in prediction of BCR after radical prostatectomy for prostate cancer.

Materials and Methods

Patients

This retrospective study was HIPAA compliant and approved by our institutional review board with a waiver of the requirement for written informed consent. A search of an institutional database to identify patients undergoing radical prostatectomy for prostate cancer who had undergone preoperative MRI at our institution between April 2011 and December 2013 yielded 432 patients. Prostate MRI was routinely performed for all patients awaiting radical prostatectomy at our institution during this time. Patients were then excluded for the following reasons: insufficient postoperative follow-up to establish a reference standard for BCR (n = 225); previous treatment of prostate cancer before MRI (n = 3); no tumor identified in prostatectomy specimen (stage pT0 tumor, n = 1) [22]; MRI performed at 1.5 T (n = 8); and severe artifact on DW images (n = 2). These exclusions left a final included cohort of 193 patients (mean age, 61 ± 7 [SD] years; range, 43–80 years). The mean preoperative PSA level was 7.7 ± 8.8 ng/mL (range, 0.8–57.0 ng/mL).

MRI Technique

All patients underwent preoperative MRI with a whole-body 3-T system (Magnetom Trio, Skya, or Verio, Siemens Healthcare) and anterior and posterior phased-array coils. Examinations included axial turbo-spin echo T2-weighted imaging (TR/TE, 4000–4960/105; slice thickness, 3 mm; FOV, 180 × 180; matrix, 256 × 256; parallel imaging factor, 2; number of signals averaged, 3) and axial fat-suppressed single-shot echo-planar DWI (TR/TE, 4100/86; slice thickness, 3 mm; FOV, 200 × 200 mm; matrix, 100 × 220; parallel imaging factor, 2; number of signals averaged, 10; b values, 50 and 1000 s/mm^2) from which the ADC map was constructed on a voxel-wide basis with a standard monoexponential fit. Dynamic contrast-enhanced imaging was performed, but the images were not reviewed as part of this study.

Image Analysis

A radiologist with 2 years of experience in prostate imaging and blinded to clinical and pathologic information evaluated images using in-house software (FireVoxel). The radiologist visually identified the lesion with the lowest ADC but did not consider any lesion with the characteristic appearance of benign prostatic hyperplasia on T2-weighted images. The radiologist then traced a 3D volume of interest (VOI) encompassing the entire lesion on the ADC map in all slices in which the lesion was visible (Fig. 1). From the VOI, the histogram of ADC values within the lesion was constructed, which in turn was used to compute the mean, entropy, kurtosis, and skewness of ADC of the entire lesion. Kurtosis characterizes the peakedness of the distribution of ADC values within the VOI such that a sharper peak indicates larger kurtosis. (The kurtosis of the whole-lesion ADC histogram in this context is a distinct metric from the diffusional kurtosis obtained through nongaussian diffusion modeling [23].) Skewness characterizes the distribution asymmetry, such that greater positive and negative skew indicate longer tails to the right and the left of the mean.

Entropy characterizes the variation in the distribution such that greater entropy indicates greater unpredictability of ADC values. In addition, adjacent nonoverlapping sections of the histogram were defined by the 10th, 25th, and 50th percentiles of the distribution. The mean ADC values of these sections were computed and denoted as $ADC_{0–10}$, $ADC_{10–25}$, and $ADC_{25–50}$. The volume of each VOI and whether the lesion was located predominantly within the peripheral zone or transition zone was also recorded.

Reference Standard

The electronic medical record was reviewed to identify PSA values obtained after radical prostatectomy. A PSA of 0.2 ng/mL or greater was considered to represent BCR [19]. For patients with BCR, the number of days from surgery to BCR was recorded. For patients without BCR, an undetectable PSA at least 1 year after the date of surgery was required for the patient to be classified as having negative findings for BCR and to be included in the analysis. For such patients, the number of days from surgery to the most recently available undetectable PSA result was recorded. Patients with either no postoperative PSA data or less than 1 year of undetectable PSA results were considered unable to be classified as having positive or negative results for BCR and were excluded from the study.

Additional information extracted from the electronic medical record for each patient included the following histopathologic features determined from assessment of the prostatectomy specimen: primary Gleason grade (classified as 3 vs > 3), overall Gleason score (classified as 6 vs > 6), perineural invasion, extraprostatic extension, seminal vesicle invasion, metastatic lymphadenopathy, and positive surgical margin. Also recorded for each patient was whether adjuvant radiation therapy was administered in the immediately postoperative period. Adjuvant radiation therapy was administered to select patients deemed at high risk of BCR on the basis of histopathologic findings, even though by definition they had an undetectable PSA level at the time of adjuvant therapy.

Statistical Analysis

Patients with and without BCR were compared by Fisher exact test for binary factors and Mann-Whitney tests for continuous factors. For binary factors with a significant association, the sensitivity and specificity for BCR were computed. For continuous factors with a significant association with BCR, the AUC from ROC curve analysis was computed along with the sensitivity and specificity at the value that maximized the Youden index subject to a constraint of a specificity of at least 70% in view of the large imbalance of patients with and without BCR. Stepwise variable selection in the context of logistic regression was used to identify sets of independent predictors of BCR from among all binary and continuous factors serving as significant predictors of BCR during the initial univariable assessments. According to the model obtained from the multivariable assessment, the AUC and the sensitivity and specificity corresponding with the model criterion maximizing the Youden index subject to a constraint of a specificity of at least 70% were computed. ROC analysis was used to compare the performance of the multivariable model with that of the individual factors in the model and with that of the model exclusive of diffusion-based metrics. Cox proportional hazards regression was used to assess the utility of the multivariable model for predicting the time to BCR, summarized by use of the Harrell concordance index (c-index).

All statistical tests were conducted at the two-sided 5% significance level with SAS software (version 9.3, SAS Institute).

Results

Clinical and Pathologic Data

At prostatectomy, the distribution of primary Gleason grades was as follows: 141 Gleason grade 3, 48 Gleason grade 4, four Gleason grade 5. The distribution of overall Gleason scores was as follows: 63 Gleason score of 6, 105 Gleason score of 7 (76 Gleason score 3 + 4, 29 Gleason score 4 + 3), 13 Gleason score of 8, and 12 Gleason score of 9. On MRI, 84% (162/193) of lesions were located predominantly within the peripheral zone. Fourty-four percent of lesions (85/193) exhibited extra-prostatic extension, 10% (20/193) had seminal vesicle invasion, 3% (6/193) exhibited metastatic lymphadenopathy, and 23% (44/193) had a positive surgical margin. Three percent (6/193) of patients received adjuvant radiation therapy in the immediate postoperative period, before documentation of a detectable PSA level. BCR subsequently developed in two of these six patients.

BCR occurred in 16.6% (32/193) of patients. In patients with BCR, the mean time from surgery to BCR was 305 ± 254 days (median, 893 days). In patients without BCR, the mean duration of a negative PSA result in postoperative follow-up was 618 ± 176 days (median, 594 days).

Univariable Assessments

Tables 1 and 2 show the results of the univariable assessments for prediction of BCR. Almost all study parameters included in the study had significant associations with BCR. Patients with BCR were significantly ($p \leq 0.019$) more likely to have a primary Gleason pattern > 3, a Gleason score > 6, extraprostatic extension, seminal vesicle invasion, perineural invasion, positive surgical margins, and metastatic lymphadenopathy. The sensitivity of these factors for prediction of BCR ranged from 15.6% (metastatic lymphadenopathy) to 96.9% (extraprostatic extension), and specificity ranged from 36.0% (perineural invasion) to 99.4% (metastatic lymphadenopathy). In addition, patients with BCR had a significantly higher preoperative PSA level, MRI tumor volume, and ADC entropy, as well as significantly lower mean ADC, $ADC_{0–10}$, $ADC_{10–25}$, and $ADC_{25–30}$ ($p \leq 0.003$). The AUC for these factors ranged from 0.66 (preoperative PSA) to 0.82 (mean ADC, $ADC_{10–25}$, and $ADC_{25–50}$) No binary or continuous variable had both sensitivity and specificity of at least 80%. Patient age, adjuvant radiation therapy, predominant peripheral zone location on MR images, and kurtosis ADC were not significantly associated with BCR ($p \geq 0.184$). Examples are shown in Figures 2 and 3.

Multivariable Assessment

Multivariable assessment identified primary Gleason grade, extraprostatic extension, $ADC_{0–10}$, and entropy ADC as significant independent predictors of BCR (Table 3). The *p* values for these factors, each adjusted for the other three parameters, ranged from 0.002 to 0.037. Together these factors had an AUC for prediction of BCR of 0.94 with sensitivity of 93.8% and specificity of 87.0%. The AUC of this model was significantly greater than the

AUC of any of the individual factors within the model alone ($p < 0.001$, all comparisons) and significantly greater than the AUC of the model when the two ADC metrics (AUC = 0.89, $p = 0.001$) were excluded. The c-index for prediction of time to BCR for the multivariable model was 0.91. Figure 4 shows the ROC curves for the multivariable model, the multivariable model without the ADC metrics, and of the individual ADC metrics.

Discussion

In this study, we developed a multivariable model for prediction of BCR of prostate cancer that combines the established clinical parameters of Gleason grade and extraprostatic extension with whole-lesion ADC metrics. Although it must be validated in external cohorts, the model had high performance within this initial cohort for prediction of both BCR (AUC, 0.94) and time until BCR (c-index, 0.91). These values compare favorably with those reported for other established models of prediction of BCR based on clinical and pathologic postprostatectomy data. For instance, studies of standard postprostatectomy algorithms have shown a c-index ranging from 0.76 to 0.82 [11, 13, 24, 25], indicating the limitations of current models. Another study integrating gene expression profiling along with standard parameters [15] showed a c-index of 0.89, although such techniques are not currently widely applied. The strong performance that we report for the model integrating standard parameters and ADC-based metrics supports a potential compelling clinical role for this approach in terms of guiding postoperative prognosis and decisions regarding adjuvant therapy.

Among the ADC metrics, $ADC_{0–10}$, but not mean ADC, was selected for inclusion in the multivariable model for prediction of BCR. In a similar fashion, Donati et al. [20] observed the 10th percentile ADC to have a significantly higher AUC than mean ADC for prediction of Gleason score. Peng et al. [26] also observed the 10th percentile ADC to have slightly higher sensitivity and specificity than mean ADC for differentiation of benign and malignant prostate tissue. In our study, the higher performance of $ADC_{0–10}$ in identifying aggressive prostate cancer may reflect the histologic heterogeneity of prostate cancer, comprising proportions of benign gland and malignant epithelium [27, 28]. In particular, among the various metrics, the mean value may be more heavily affected by intermixed benign tissue, whereas the $ADC_{0–10}$ may more strongly reflect focal regions of aggressive elements within the overall tumor volume [20].

In addition to $ADC_{0–10}$, entropy ADC was a significant independent predictor of ADC. Its role as an independent predictor can be attributed to its distinct nature in comparison with the other ADC metrics identified at univariable evaluation. Entropy reflects tissue heterogeneity, being influenced by variability and predictability of ADC values within the histogram [21]. A past study [21] showed that ADC entropy has a stronger association with the percentage Gleason 4 component within prostate tumors than mean ADC does. Given its complex derivation and reflection of overall lesion texture, lesion entropy cannot be approximated on the basis of qualitative image assessment or a focal ROI evaluation with a standard clinical PACS. Rather, this parameter generally entails whole-lesion analysis with dedicated image analysis software. As data continue to emerge in support of the prognostic

value of whole-lesion histogram-based assessment, such methods may become more routine in clinical practice.

Past studies have also explored associations between MRI findings and BCR. Park et al. [19] observed mean ADC from a single-slice ROI to have an AUC of 0.755 for prediction of BCR, although no model combining mean ADC with clinical or pathologic parameters could be identified. More recently, Park et al. [29] described a multivariable model combining standard clinical factors and the mere qualitative presence of visible tumor on MR images; however, the overall accuracy, sensitivity, and specificity of the multivariable model constructed in that study were not reported [29]. Other, more remote studies based on subjective MRI assessments [30, 31] did not show significant improvements in prognostic accuracy through MRI findings. On this basis, the more advanced quantitative analysis used in our study appears to be an important component of optimizing the potential utility of MRI in prostate cancer risk assessment.

A number of limitations of our study warrant mention. First, this was a retrospective study, with a small number of patients with positive results for BCR. In addition, the minimum follow-up interval for considering patients not to have BCR was 12 months. Although this matches the minimum follow-up interval applied in a previous study of prediction of BCR [19], it is expected that a fraction of these patients would have had BCR with longer surveillance. Furthermore, we included patients who had undergone adjuvant radiation therapy. Current national consensus guidelines advise offering such treatment to patients with high-risk pathologic features of BCR [10], so exclusion of such patients would have caused our model not to apply to a subset of patients at highest risk of the outcome of interest. Nonetheless, the rate of adjuvant radiation therapy in our cohort was low. This may relate to the frequent use at our institution of early salvage therapy [9, 32]. Moreover, although preoperative radiation therapy has been used in nomograms for prediction of BCR [33], we excluded patients with preoperative treatment because of the potential effect of such therapy on ADC values. Another limitation was the exclusion of approximately one half of patients undergoing prostatectomy at our institution during the study interval owing to insufficient PSA follow-up, potentially biasing the results. In addition, interreader reproducibility of the whole-lesion ADC metrics was not assessed. Finally, our observations require validation in separate independent cohorts to establish the generalizability of the model.

Conclusion

We developed a multivariable model combining primary Gleason grade, extraprostatic extension, and both $ADC_{0–10}$ and entropy ADC from whole-lesion tumor assessment in prediction of BCR of prostate cancer. Together these factors had excellent performance within this initial cohort, achieving an AUC of 0.94. The selection of these two ADC metrics, but not of standard mean ADC, for inclusion in the model indicates the value of whole-lesion histogram analysis for optimizing characterization of tumor aggressiveness. This multivariable model may have clinical application in postoperative assessments of prognosis and treatment decisions. Future validation in independent cohorts remains warranted.

Acknowledgments

S. S. Taneja is a consultant for Hitachi-Aloka and for Healthtronics, receives payments for lectures and travel and accommodation expenses from Hitachi-Aloka, and receives royalties from Elsevier.

Supported by the Joseph and Diane Steinberg Charitable Trust.

References

1. Bill-Axelson A, Holmberg L, Garmo H, et al. Radical prostatectomy or watchful waiting in early prostate cancer. N Engl J Med. 2014; 370:932–942. [PubMed: 24597866]
2. Hull GW, Rabbani F, Abbas F, Wheeler TM, Kattan MW, Scardino PT. Cancer control with radical prostatectomy alone in 1,000 consecutive patients. J Urol. 2002; 167:528–534. [PubMed: 11792912]
3. Freedland SJ, Humphreys EB, Mangold LA, Eisenberger M, Partin AW. Time to prostate specific antigen recurrence after radical prostatectomy and risk of prostate cancer specific mortality. J Urol. 2006; 176:1404–1408. [PubMed: 16952644]
4. Pound CR, Partin AW, Eisenberger MA, Chan DW, Pearson JD, Walsh PC. Natural history of progression after PSA elevation following radical prostatectomy. JAMA. 1999; 281:1591–1597. [PubMed: 10235151]
5. Lohm G, Lütcke J, Jamil B, et al. Salvage radiotherapy in patients with prostate cancer and biochemical relapse after radical prostatectomy: long-term follow-up of a single-center survey. Strahlenther Onkol. 2014; 190:727–731. [PubMed: 24577132]
6. Kwon O, Kim KB, Lee YI, et al. Salvage radiotherapy after radical prostatectomy: prediction of biochemical outcomes. PLoS One. 2014; 9:e103574. [PubMed: 25072938]
7. Botticella A, Guarneri A, Levra NG, et al. Biochemical and clinical outcomes after high-dose salvage radiotherapy as monotherapy for prostate cancer. J Cancer Res Clin Oncol. 2014; 140:1111–1116. [PubMed: 24744191]
8. Wiegel T, Bartkowiak D, Bottke D, et al. Adjuvant radiotherapy versus wait-and-see after radical prostatectomy: 10-year follow-up of the ARO 96-02/AUO AP 09/95 trial. Eur Urol. 2014; 66:243–250. [PubMed: 24680359]
9. Pearse M, Fraser-Browne C, Davis ID, et al. A phase III trial to investigate the timing of radiotherapy for prostate cancer with high-risk features: background and rationale of the Radiotherapy–Adjuvant Versus Early Salvage (RAVES) trial. BJU Int. 2014; 113(suppl 2):7–12. [PubMed: 24894850]
10. Kalbasi A, Swisher-McClure S, Mitra N, et al. Low rates of adjuvant radiation in patients with nonmetastatic prostate cancer with high-risk pathologic features. Cancer. 2014; 120:3089–3096. [PubMed: 24917426]
11. Swanson GP, Yu C, Kattan MW, Hermans MR. Validation of postoperative nomograms in prostate cancer patients with long-term follow-up. Urology. 2011; 78:105–109. [PubMed: 21507467]
12. Eggener SE, Vickers AJ, Serio AM, et al. Comparison of models to predict clinical failure after radical prostatectomy. Cancer. 2009; 115:303–310. [PubMed: 19025977]
13. Stephenson AJ, Scardino PT, EasthAm JA, et al. Postoperative nomogram predicting the 10-year probability of prostate cancer recurrence after radical prostatectomy. J Clin Oncol. 2005; 23:7005–7012. [PubMed: 16192588]
14. Shariat SF, Karakiewicz PI, Roehrborn CG, Kattan MW. An updated catalog of prostate cancer predictive tools. Cancer. 2008; 113:3075–3099. [PubMed: 18823041]
15. Stephenson AJ, Smith A, Kattan MW, et al. Integration of gene expression profiling and clinical variables to predict prostate carcinoma recurrence after radical prostatectomy. Cancer. 2005; 104:290–298. [PubMed: 15948174]
16. Hambrock T, Somford DM, Huisman HJ, et al. Relationship between apparent diffusion coefficients at 3.0-T MR imaging and Gleason grade in peripheral zone prostate cancer. Radiology. 2011; 259:453–461. [PubMed: 21502392]

17. Kobus T, Vos PC, Hambrock T, et al. Prostate cancer aggressiveness: in vivo assessment of MR spectroscopy and diffusion-weighted imaging at 3 T. Radiology. 2012; 265:457–467. [PubMed: 22843767]
18. Hoeks CM, Vos EK, Bomers JG, Barentsz JO, Hulsbergen-van de Kaa CA, Scheenen TW. Diffusion-weighted magnetic resonance imaging in the prostate transition zone: histopathological validation using magnetic resonance-guided biopsy specimens. Invest Radiol. 2013; 48:693–701. [PubMed: 23614975]
19. Park SY, Kim CK, Park BK, Lee HM, Lee KS. Prediction of biochemical recurrence following radical prostatectomy in men with prostate cancer by diffusion-weighted magnetic resonance imaging: initial results. Eur Radiol. 2011; 21:1111–1118. [PubMed: 21046403]
20. Donati OF, Mazaheri Y, Afaq A, et al. Prostate cancer aggressiveness: assessment with whole-lesion histogram analysis of the apparent diffusion coefficient. Radiology. 2014; 271:143–152. [PubMed: 24475824]
21. Rosenkrantz AB, Triolo MJ, Melamed J, Rusinek H, Taneja SS, Deng FM. Whole-lesion apparent diffusion coefficient metrics as a marker of percentage Gleason 4 component within Gleason 7 prostate cancer at radical prostatectomy. J Magn Reson Imaging. 2015; 41:708–714. [PubMed: 24616064]
22. Gross JL, Masterson TA, Cheng L, Johnstone PA. pT0 prostate cancer after radical prostatectomy. J Surg Oncol. 2010; 102:331–333. [PubMed: 20589707]
23. Kierans AS, Bennett GL, Mussi TC, et al. Characterization of malignancy of adnexal lesions using ADC entropy: comparison with mean ADC and qualitative DWI assessment. J Magn Reson Imaging. 2013; 37:164–171. [PubMed: 23188749]
24. Walz J, Chun FK, Klein EA, et al. Nomogram predicting the probability of early recurrence after radical prostatectomy for prostate cancer. J Urol. 2009; 181:601–607. discussion 607–608. [PubMed: 19084864]
25. Kang M, Jeong CW, Choi WS, et al. Pre- and post-operative nomograms to predict recurrence-free probability in Korean men with clinically localized prostate cancer. PLoS One. 2014; 9:e100053. [PubMed: 24936784]
26. Peng Y, Jiang Y, Yang C, et al. Quantitative analysis of multiparametric prostate MR images: differentiation between prostate cancer and normal tissue and correlation with Gleason score—a computer-aided diagnosis development study. Radiology. 2013; 267:787–796. [PubMed: 23392430]
27. Langer DL, van der Kwast TH, Evans AJ, et al. Intermixed normal tissue within prostate cancer: effect on MR imaging measurements of apparent diffusion coefficient and T2-sparse versus dense cancers. Radiology. 2008; 249:900–908. [PubMed: 19011187]
28. Rosenkrantz AB, Mendrinos S, Babb JS, Taneja SS. Prostate cancer foci detected on multiparametric magnetic resonance imaging are histologically distinct from those not detected. J Urol. 2012; 187:2032–2038. [PubMed: 22498205]
29. Park JJ, Kim CK, Park SY, Park BK, Lee HM, Cho SW. Prostate cancer: role of pretreatment multiparametric 3-T MRI in predicting biochemical recurrence after radical prostatectomy. AJR. 2014; 202:W459–W465. [web]. [PubMed: 24758681]
30. Fuchsjäger MH, Shukla-Dave A, Hricak H, et al. Magnetic resonance imaging in the prediction of biochemical recurrence of prostate cancer after radical prostatectomy. BJU Int. 2009; 104:315–320. [PubMed: 19220263]
31. D'Amico AV, Whittington R, Malkowicz B, et al. Endorectal magnetic resonance imaging as a predictor of biochemical outcome after radical prostatectomy in men with clinically localized prostate cancer. J Urol. 2000; 164:759–763. [PubMed: 10953141]
32. Briganti A, Wiegel T, Joniau S, et al. Early salvage radiation therapy does not compromise cancer control in patients with pT3N0 prostate cancer after radical prostatectomy: results of a match-controlled multi-institutional analysis. Eur Urol. 2012; 62:472–487. [PubMed: 22633803]
33. Memorial Sloan Kettering Cancer Center website. Prediction tools: prostate cancer—post-radical prostatectomy. nomograms.mskcc.org/Prostate/PostRadicalProstatectomy.aspx.

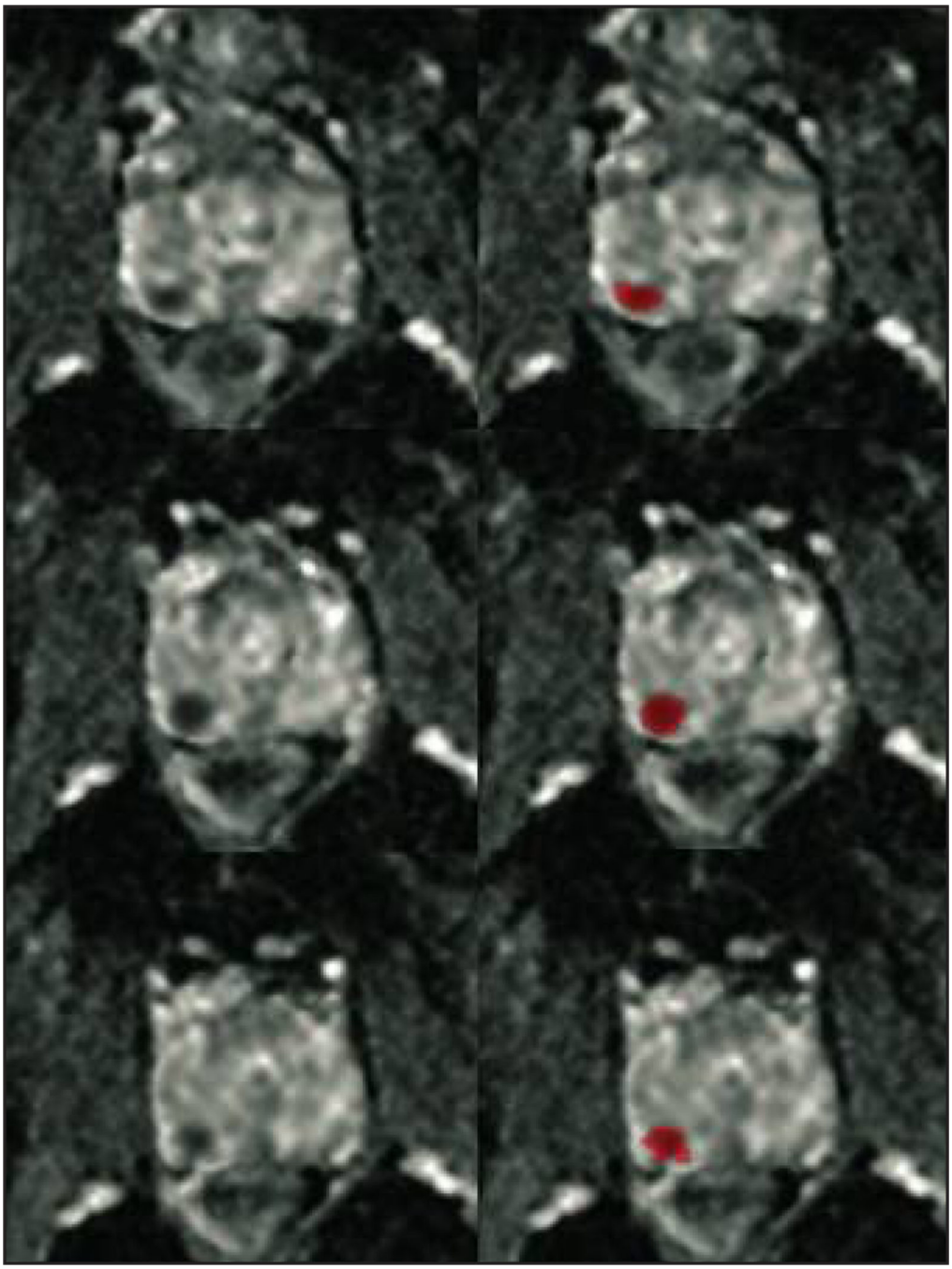

Fig. 1.

52-year-old man with prostate cancer. Consecutive axial slices from apparent diffusion coefficient (ADC) map show area of decreased ADC in right posterior peripheral zone (*left*) and 3D volume of interest encompassing area of low ADC (*red*) in each slice (*right*).

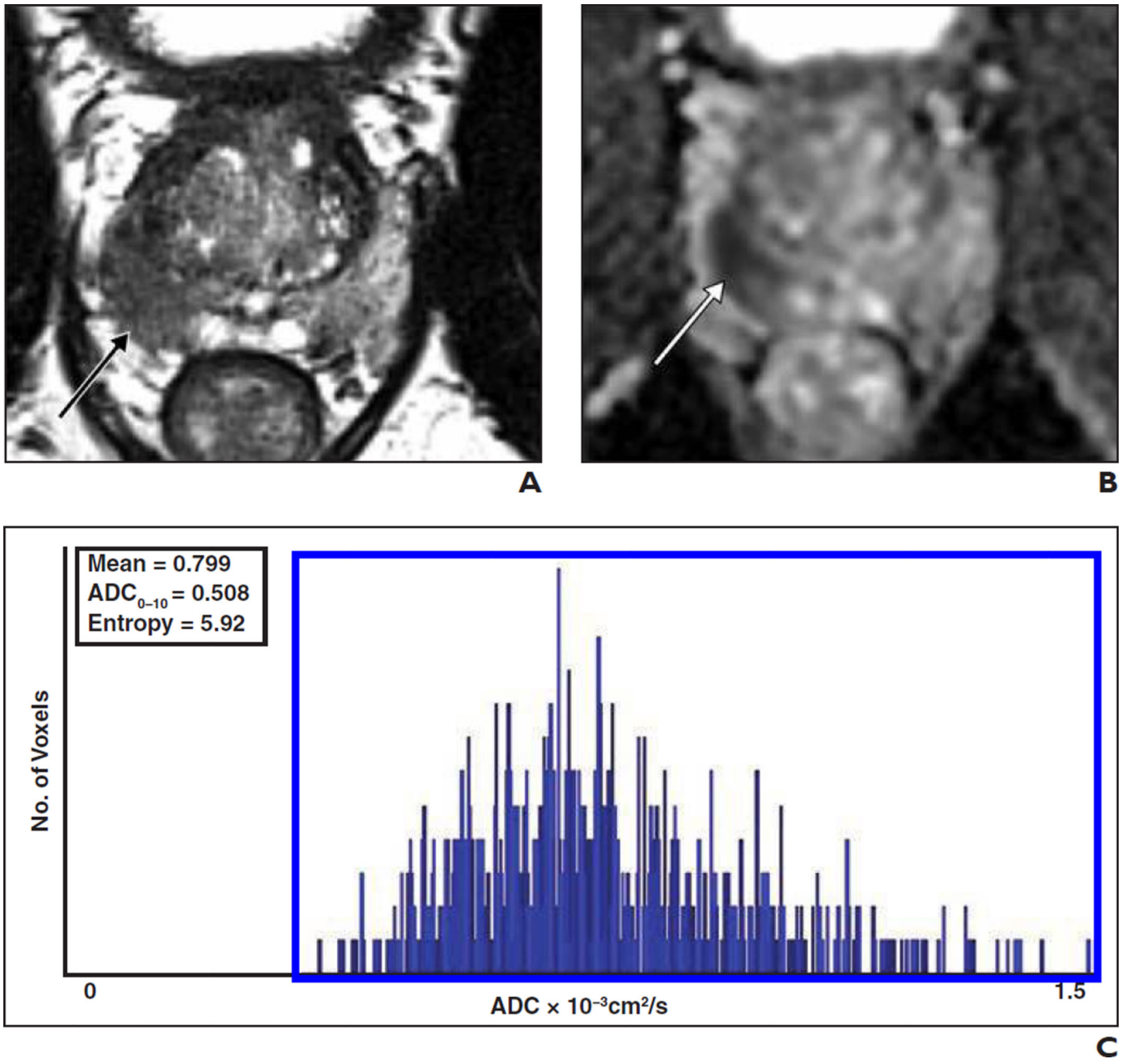

Fig. 2.

63-year-old man with prostate cancer and preoperative prostate-specific antigen level of 4.96 ng/mL. Pathologic assessment of prostatectomy specimen showed Gleason 3 + 4 tumor with extraprostatic extension but no seminal vesicle invasion. Biochemical recurrence occurred 310 days postoperatively.

A, Axial turbo spin-echo T2-weighted MR image shows area of decreased T2 signal intensity (*arrow*) in right peripheral zone.

B, Axial apparent diffusion coefficient (ADC) map shows area of decreased ADC (*arrow*) corresponding to area of decreased signal intensity in **A**.

C, Histogram of whole-lesion volume of interest placed on ADC map shows derived whole-lesion metrics, including low mean ADC, low ADC for 10th percentile ($ADC_{0–10}$), and relatively high ADC entropy compared with overall status cohort.

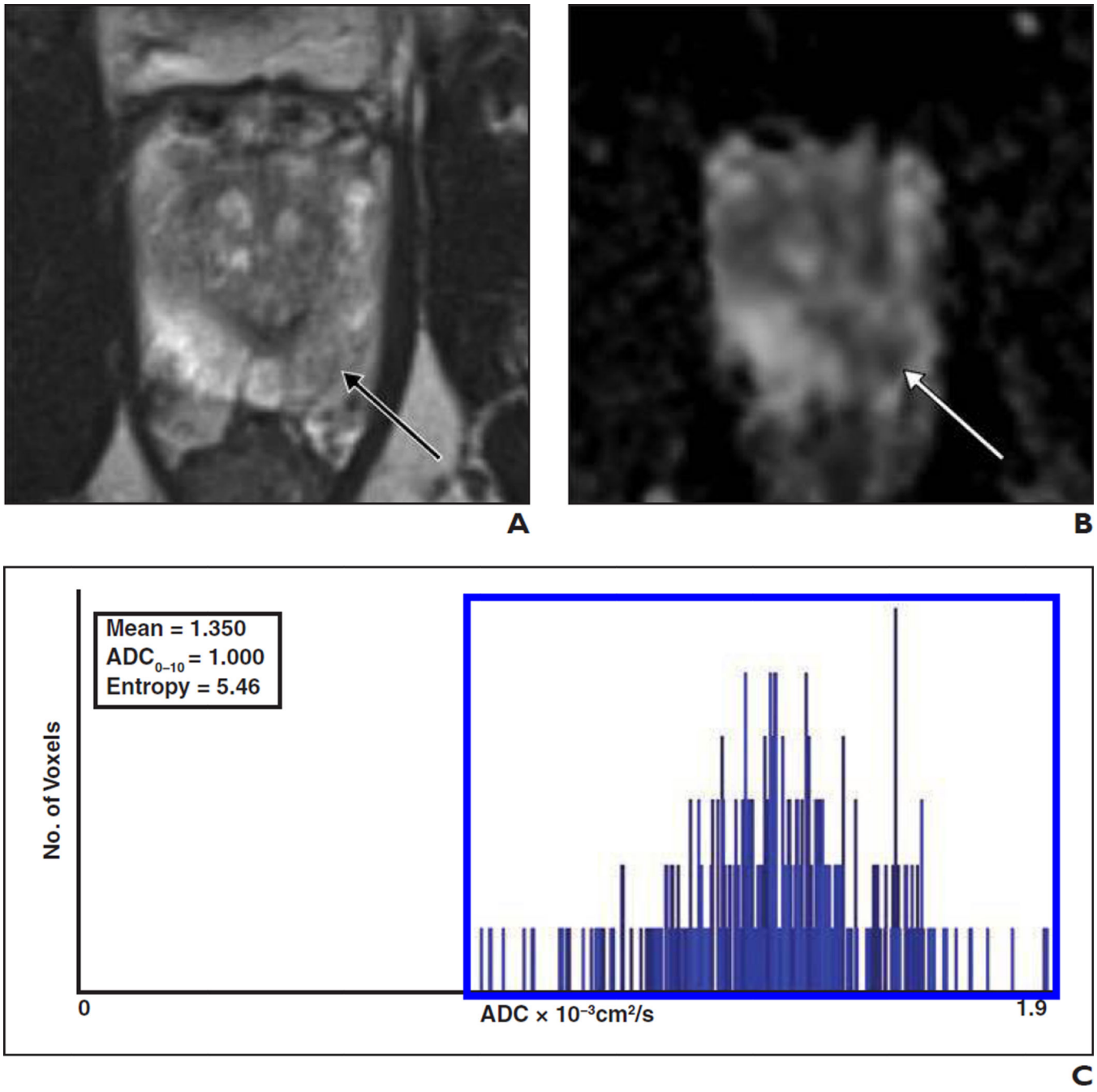

Fig. 3.

56-year-old man with prostate cancer and preoperative prostate-specific antigen (PSA) level of 6.0 ng/mL. Pathologic assessment of prostatectomy specimen showed Gleason 4 + 3 tumor without extraprostatic extension or seminal vesicle invasion. PSA remained undetectable 690 days postoperatively.

A, Axial turbo spin-echo T2-weighted MR image shows area of geographic mildly decreased T2 signal intensity (*arrow*) in left apical posterior peripheral zone.

B, Axial apparent diffusion coefficient (ADC) map shows area of decreased ADC (*arrow*) corresponding to area of low signal intensity in **A**.

C, Histogram of whole-lesion volume of interest placed on ADC map shows derived whole-lesion metrics, including high mean ADC, high ADC for 10th percentile ($ADC_{0–10}$), and relatively low ADC entropy compared with overall status cohort.

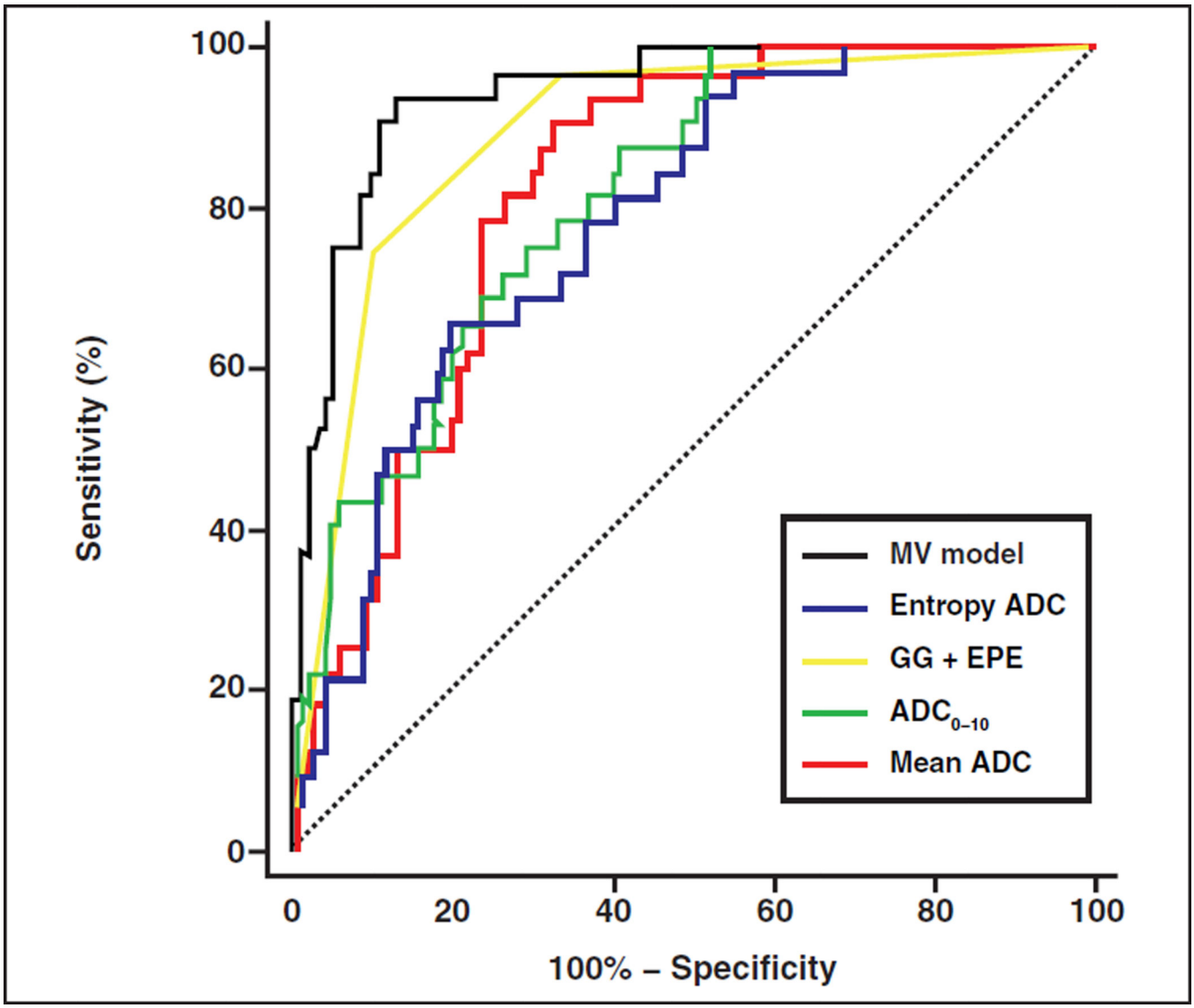

Fig. 4.

Graph shows ROC curves of multivariable (MV) model comprising entropy apparent diffusion coefficient (ADC), primary Gleason grade (GG), extraprostatic extension (EPE), and ADC for 10th percentile ($ADC_{0–10}$); multivariable model without ADC metrics (GG + EPE); and individual ADC metrics included in model. Highest performance is for multivariable model combining pathologic and whole-lesion ADC metrics.

TABLE 1

Summary of Binary Factors Identified as Having Statistically Significant Associations With Biochemical Recurrence at Univariable Analysis

Factor	Sensitivity (%)	Specificity (%)	*p*
Primary Gleason grade (3 vs > 3)	75.0 (24/32)	82.6 (133/161)	< 0.001
Gleason score (6 vs > 6)	100 (32/32)	39.1 (63/161)	< 0.001
Extraprostatic extension	96.9 (31/32)	66.5 (107/161)	< 0.001
Seminal vesicle invasion	37.5 (12/32)	95.0 (153/161)	< 0.001
Perineural invasion	90.6 (29/32)	36.0 (58/161)	0.003
Positive surgical margin	40.6 (13/32)	80.7 (130/161)	0.019
Metastatic lymphadenopathy	15.6 (5/32)	99.4 (160/161)	0.001

Note—Remaining binary factors (predominant peripheral zone location on MR images and adjuvant radiation therapy) not identified as having significant associations ($p \geq 0.184$).

TABLE 2

Summary of Continuous Factors Identified as Having Significant Associations With Biochemical Recurrence at Univariable Analysis

Factor	No Biochemical Recurrence	Biochemical Recurrence	*p*	AUC	Optimal Threshold	Sensitivity (%)	Specificity (%)
Preoperative prostate-specific antigen level (ng/mL)	6.7 ± 6.7	12.7 ± 12.8	0.003	0.66	> 6.3	59.4	72.5
MRI tumor volume (cm^3)	1.36 ± 1.53	4.10 ± 5.69	< 0.001	0.78	> 1.92	62.5	83.2
Mean ADC ($\times 10^{-3}$ mm^2/s)	1.08 ± 0.0.25	0.81 ± 0.16	< 0.001	0.82	≤ 0.94	81.3	73.3
$ADC_{0–10}$ ($\times 10^{-3}$ mm^2/s)	0.74 ± 0.27	0.42 ± 0.0.22	< 0.001	0.81	≤ 0.52	65.6	78.9
$ADC_{10–25}$ ($\times 10^{-3}$ mm^2/s)	0.89 ± 0.27	0.59 ± 0.19	< 0.001	0.82	≤ 0.65	62.5	81.4
$ADC_{25–50}$ ($\times 10^{-3}$ mm^2/s)	1.01 ± 0.26	0.73 ± 0.17	< 0.001	0.82	≤ 0.84	71.9	75.8
Entropy ADC	5.38 ± 0.61	5.98 ± 0.44	< 0.001	0.78	> 5.85	65.6	80.1

Note—Remaining continuous factors (patient age, ADC kurtosis, and ADC skewness) not identified as having significant associations ($p \geq 0.333$). ADC = apparent diffusion coefficient.

TABLE 3

Factors Included in Multivariable Model for Prediction of Biochemical Recurrence

Factor	Adjusted *p*
Primary Gleason grade	0.005
Extraprostatic extension	0.004
Mean ADC of the bottom 10^{th} percentile ($\times 10^{-3}$ mm^2/s)	0.002
Entropy ADC	0.037

Note—Adjusted for other factors within model. Model showed AUC of 0.94 for prediction of biochemical recurrence. ADC = apparent diffusion coefficient.